Role of Kinks in the Dynamics of Contact Lines Receding on Superhydrophobic Surfaces

Anaïs Gauthier, Marco Rivetti, Jérémie Teisseire, and Etienne Barthel

Surface du Verre et Interfaces, UMR 125 CNRS/Saint-Gobain, 39 Quai Lucien Lefranc, F-93303 Aubervilliers, Cedex, France (Received 16 October 2012; revised manuscript received 4 December 2012; published 25 January 2013)

We have investigated the depinning of the contact line on superhydrophobic surfaces with anisotropic periodic textures. By direct observation of the contact line conformation, we show that the mobility is mediated by kink defects. Full 3D simulations of the shape of the liquid surface near the solid confirm that kinks account for the measured wetting properties. This behavior, which is similar to the Peierls-Nabarro mechanism for dislocations, may open perspectives for the optimization of wetting hysteresis by design.

DOI: 10.1103/PhysRevLett.110.046101 PACS numbers: 68.08.Bc, 47.55.D-

In the quest for water repellent surfaces, the benefit of surface textures has been emphasized for decades [1–5]. When a droplet is suspended on surface textures, the actual area of contact between the liquid and the solid is reduced. The ratio of the actual area of contact to the total area is the solid fraction $\phi < 1$. It is tempting to assume a proportional reduction of the work of adhesion of the liquid w; this is the Cassie theory [6] which predicts the well-known rule of mixture: $w/\gamma \equiv (1+\cos\theta) = \phi(1+\cos\theta_0)$ where θ is the contact angle on the textured surface, θ_0 the contact angle on the flat surface and γ the surface energy of the liquid. This thermodynamic approach, which emulates the standard derivation of the Young equation [7], simply proceeds by areal averaging of the surface energies.

One obvious limitation of the Cassie theory is that it predicts only one contact angle. However, the contact angle for a wetting liquid (advancing) is usually quite different from the contact angle for dewetting (receding). Contrasted advancing and receding contact angles result in a sticky surface, which defeats the claim to water repellency. Strong emphasis has recently been laid on this contact angle hysteresis, and the failure of the Cassie equation in this respect has been highlighted [8]. Indeed the Cassie theory assumes that the contact line statistically explores all configurations on the heterogeneous surface. However at the scale of the texture, the deformation energy of the liquid surface is considerably larger than the thermal energy [7]. Large heterogeneities induce pinning, instabilities, and hysteresis. This is a generic behavior, which is found not only in wetting [9], but also in many other systems ranging from fracture [10] to spin density waves [11].

Several methods have been developed to circumvent this shortcoming of the Cassie theory. Thresholds for line instabilities can be approximated by averaging over the perimeter of the contact line [12–14]. One of the most successful methods is the differential area theory proposed by Choi *et al.* [13] where energy extrema are estimated for specific configurations of the contact line. They indeed correctly predict the scaling of the receding contact angle with the lattice parameter for square arrays.

However there remains some conceptual difficulties: energy averages over the contact line depend on the configuration of the line at instability, and this configuration is not predicted by the theory. As a result, most often, for periodic surfaces, we consider a macroscopically straight segment of the (locally wavy) contact line [Fig. 1(a)]. Assuming such a straight contact line, the differential area theory predicts that the receding contact angles should be different along inequivalent rows. However, Dorrer and Rühe [15] have measured the wetting properties of anisotropic surfaces: they found very limited anisotropy for the receding contact angle. On surfaces textured with stripes, which are even more anisotropic, Choi et al. [13] also evidenced isotropic receding contact angles. To explain this result, they implicitly discard the straight line assumption: they show that the local motion of the contact line takes place along the stripes, even when the line macroscopically moves in the normal direction. This case highlights the limitation of the differential area method: for stripes the relevant conformation is relatively easy to guess, but for less symmetric surfaces, the theory does not provide the line conformation at instability and efficient prediction of contact angles is still elusive.

In the present experiments we have generalized the stripe geometry proposed by Choi et al. [13] following

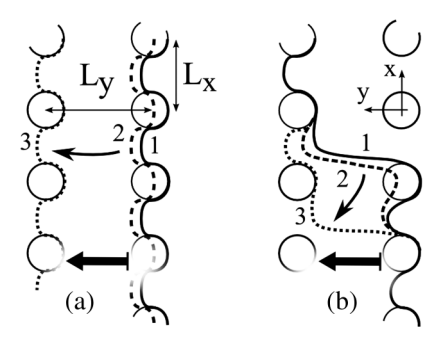


FIG. 1. Schematics of a contact line receding: (a) as a straight segment on a rectangular array and (b) as a kink. The sequence of lines 1,2, and 3 suggests the kinematics of depinning for each configuration.

Dorrer and Rühe [15]. We have systematically characterized the motion of the contact line on rectangular post arrays (Fig. 1) as a function of lattice parameters: we have measured receding contact angles for lines propagating in the *x* and *y* directions and we have monitored the propagation mechanism through direct observations. The results demonstrate that the kinematics is determined by the motion of kinks in the contact line [Fig. 1(b)], in contrast to the straight line assumption. Numerical simulations confirm the impact of the kinks on contact line dynamics and quantitatively support our conclusion.

Hybrid silica layers were spin-coated on glass substrates using a sol-gel process, and the surface textures were imprinted with elastomeric stamps as described previously [16]. The surfaces exhibit rectangular post arrays with constant post size (diameter 12.5 μ m \pm 1.0, height 11 μ m). The lattice parameter L_x was kept constant at 20 μ m while L_y was varied between 20 and 70 μ m (Fig. 1). The wetting properties of the hybrid silica material were characterized: for the flat surface advancing and receding contact angles are, respectively, $\theta_{0,adv} = 119 \pm 3^\circ$ and $\theta_{0,rec} = 89 \pm 3^\circ$.

The contact angle measurements were carried out with a DSA100 goniometer (Krüss, Germany) in dynamic mode (drop volume oscillating between 6 and 12 μ l) and the data processed with the ImageJ plugin. The surface was rotated by 90° to measure both x and y directions. We find that the receding contact angles (Fig. 2) decrease with the solid fraction. The dependence with the lattice parameter L_y is very similar to the behavior previously observed for square lattices [17], and quite different from the Cassie predictions [13,16]. Our values are also fully consistent with the findings of Dorrer and Rühe [15]: we observe that wetting anisotropy is very limited for the full range of lattice parameters explored. Even strongly anisotropic surfaces result in nearly isotropic receding contact angles.

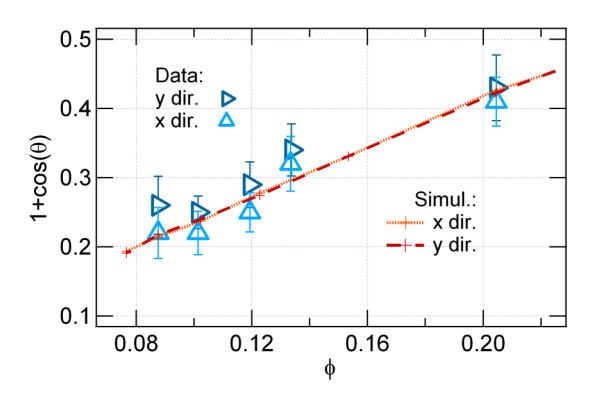


FIG. 2 (color online). Measured receding contact angles for various lattice parameters, plotted as normalized work of adhesion as a function of the solid fraction. The two directions x and y are shown. Contact angles calculated from full 3D simulations of depinning are also shown, for $w_0 = 1.45$ (see text).

To understand this behavior, we investigated the conformation of the contact line in detail during evaporation. As with polymeric materials [18], the contact can easily be monitored by optical microscopy through the transparent substrate (Fig. 3, top; for a video see the Supplemental Material [19]). A sequence of snapshots of the contact line near the y edge of the contact area (Fig. 3, bottom) summarizes our observations of the motion. Macroscopically the contact line moves in the y direction. Microscopically what is seen is the quicker, jerky motion along x of small perpendicular contact line segments joining two dense rows. This local motion at the post length scale is schematized in Fig. 1(b). These features are similar to the "jogs" described by de Gennes [7] for stripes, and were very clearly anticipated by Dorrer and Rühe [15]. We think they can be more aptly called kinks in the context of arrays, as further discussed below. The kinematics of the kinks is especially visible when the front propagates in the y direction, due to the larger kink width, but we have found that kinks account for contact line motion all around the drop, and on all the surfaces investigated here.

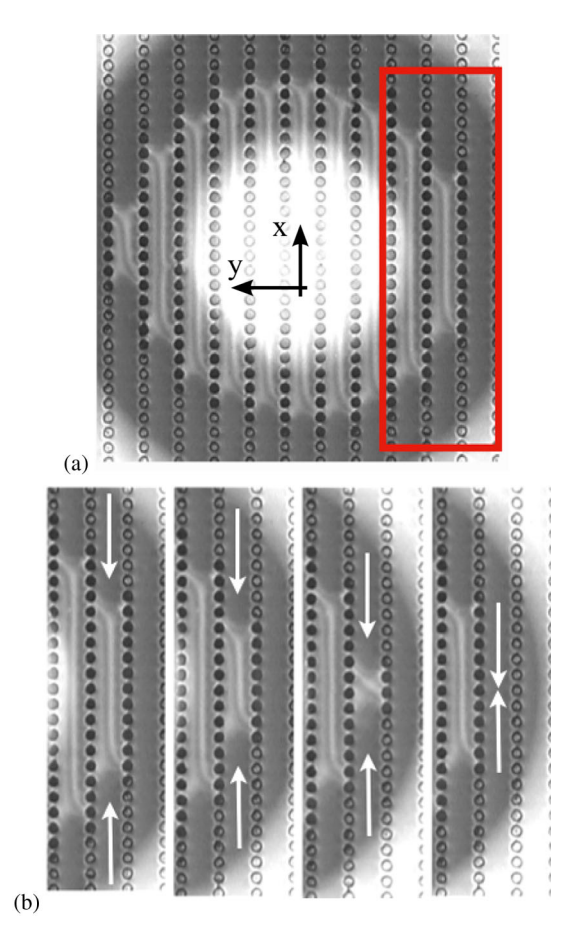


FIG. 3 (color online). Direct visualization of the motion of the contact line on a rectangular array with $L_x = 20~\mu m$ and $L_y = 50~\mu m$: (a) full view of the contact area and (b) a sequence of depinning events, showing the succession of kink motions. The rectangular box in (a) marks the location of the sequence (b).

As a next step we have simulated the depinning of the contact line to evaluate the impact of kinks on (1) the anisotropy of the wetting properties, and (2) the dependence of the receding contact angle on the solid fraction. Using the powerful minimization algorithm SURFACE EVOLVER [20], we calculated a minimal surface obeying the relevant boundary conditions. For the straight line we simulated a periodic row. The unit cell consists of two posts: the contact line sits on the first post, while the second post is located further back. Only the front post turns out to be active during depinning. For kinks we used a six-post configuration (Fig. 4, inset) with two extensions at the continuum level of description on the sides to avoid spurious boundary condition effects. Once the geometry of the textures (post diameter and lattice parameters) and the work of adhesion of the liquid on the post surface $w_0 = \gamma(1 + \cos\theta_{0,\text{rec}})$ are specified, we can accurately calculate the contact line conformation, or more exactly the full shape of the liquid surface near the solid. A typical result for a receding contact line is shown in Fig 4; note the close similarity with the direct observations with scanning electron microscopy [21]. For quantitative evaluation of the wetting properties, we adjust the contact angle θ_{wall} of the liquid on some arbitrary upper interface, parallel to the solid and far above (typically 10 times the unit cell size) [22] (Fig 4). Gradually increasing this contact angle increases the loading on the contact line until dewetting is initiated on the most sensitive post. The angle is increased further until the contact line becomes unstable and the post is fully dewetted: this event determines the macroscopic receding contact angle $\theta_{\rm rec} = \pi - \theta_{\rm wall}$ of the textured surfaces.

We have modeled a nominal surface with post diameter $10 \ \mu m$ and $\theta_{0,rec} = 90^{\circ}$ for a large range of lattice parameters. The resulting receding contact angles are plotted as a function of ϕ in Fig. 5. For the straight line simulations [Fig. 1(a)] we evidence strong anisotropy as

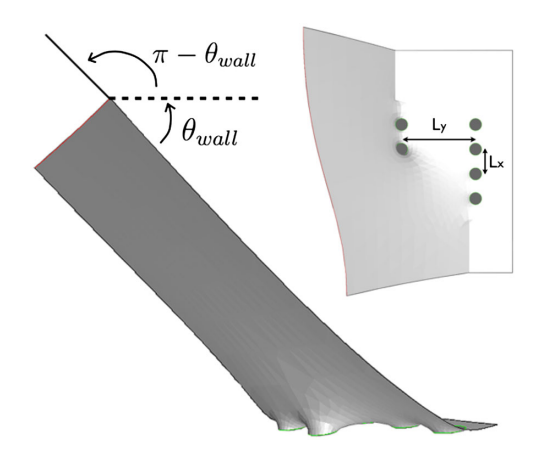


FIG. 4 (color online). Simulation of the depinning event for a contact line with a kink. The equilibrium minimal surface is shown just before depinning occurs. Inset: Top view of geometry of the surface.

expected: if the line propagates in the y direction the result is quite naturally independent of L_y . On the other hand, if the line propagates in the x direction, the result depends strongly on L_y and the work of adhesion $1 + \cos\theta_{\rm rec}$ decreases with ϕ as observed. The differential area model [13] is also shown, and we note an excellent agreement with the straight line simulations.

Following the previous reasoning on stripes, we would expect the receding contact angle for propagation along x (the easier direction) to rule dewetting on these surface. However, the simulations show that the receding contact angle increases further—and the work of adhesion decreases—when a kink is introduced in the line (Fig. 5). For larger solid fractions, in the experimentally accessible range, the threshold with a kink is about 2/3 lower than the threshold for a straight line. In addition, we find that with a kink, within numerical errors, the receding contact angle is the same in the x and the y direction of propagation. These results are completely consistent with our direct observations of the contact line which evidence that contact line propagation proceeds through the motion of kinks, not straight lines. Since the threshold is the same in both directions, receding contact angles do not depend upon the orientation of the contact line: surface anisotropy is suppressed and the drop maintains a quasicircular shape even on geometrically anisotropic surfaces.

To further substantiate these predictions experimentally, we have fabricated two surfaces with identical local morphology but different topology. The first surface is one of our usual rectangular arrays, with $L_x = 30 \ \mu \text{m}$, $L_y = 40 \ \mu \text{m}$ and pillar diameter 14 μm . On this surface a droplet develops a circular contact line with a distribution of kinks similar to Fig. 3. The receding contact angles were found to reach about 132°. More precisely the normalized effective work of adhesion $1 + \cos(\theta_{\text{rec}}) = 0.32 \pm 0.04$ in the x direction and 0.34 ± 0.03 in the y direction, consistent with the data in Fig. 2. The other surface is textured

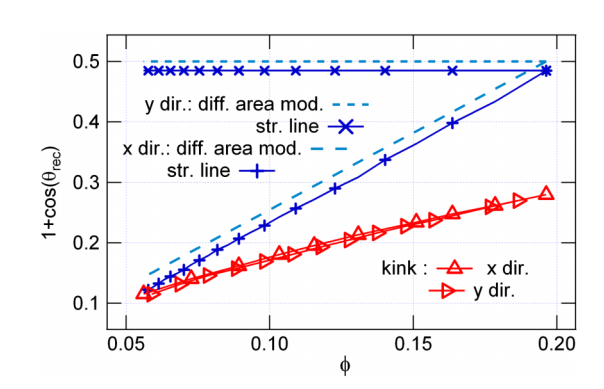


FIG. 5 (color online). Computed receding contact angles plotted as effective work of adhesion vs the solid fraction, with $w_0 = 1.0$. Computed values for the straight line are compared to results of the differential area model and to computed values with a kink.

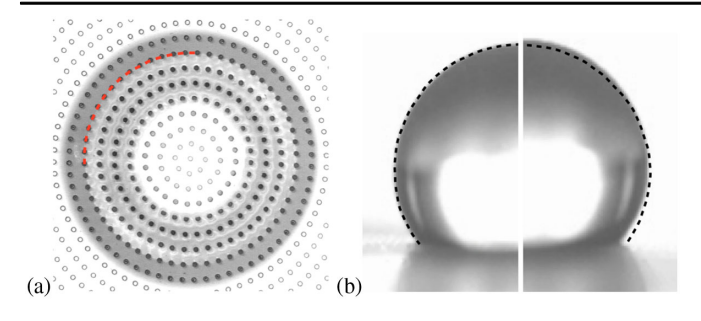


FIG. 6 (color online). (a) Pillar loop with a pinned contact line, and (b) droplet just before [(b), left] and just after [(b), right] instability. The contact angle at instability is lower than the contact angle on the rectangular array because of the absence of kinks.

with circular loops of pillars [Fig. 6(a)]. The layout has been designed so as to maintain a local geometry similar to the rectangular array, with nearly identical spacings between pillars. However, the topology of the circle can match the drop shape: when a drop is deposited near the center of the loop, it self-centers during evaporation. The contact line anneals itself until a circular, kink-free contact line is stabilized [Fig. 6(a)]. This contact line is pinned [Fig. 6(b), left] and the contact angle decreases with further evaporation, until at about 121.5° [and an effective normalized work of adhesion $1 + \cos(\theta_{\rm rec}) = 0.48 \pm 0.01$] an instability rapidly develops all around the droplet which pops in, into the next row [Fig. 6(b), right]. The contrast between effective works of adhesion for the kink-free contact line and the contact line with kinks lies quite close to the 2/3 ratio predicted by the simulations.

In brief, kinks do control line motion on periodic superhydrophobic surfaces: they reduce the threshold for depinning of the contact line and produce isotropic wetting properties. If the kinks are suppressed, as with pillar loops, straight line jumps are observed, with a larger depinning threshold. Turning back to the experiments by Choi *et al.* [13] on striped surfaces, and especially on spirals, we note that the transverse contact line spanning two consecutive rows (Fig. 5d in their paper)—de Gennes' "jog" [7]—is effectively a kink. It is no surprise that it is found to play a central role for receding contact lines; indeed, for stripes, at the continuum limit, the threshold is expected to be nil [7], as observed experimentally [13].

However, we note that, starting from a reasonable value $\theta_{0,\rm rec}=90^\circ$, the receding contact angles we evaluate for a contact line with a kink (Fig. 5) do not fall on the data (Fig. 2). In fact, a good fit to the kink model is only obtained by increasing the work of adhesion of the liquid from 1 to 1.45, a value which is equivalent to an effective contact angle $\theta_{0,\rm rec}=63^\circ$ on the flat surface (Fig. 2). We do not have a definite explanation for this discrepancy, but it has recently been demonstrated experimentally that contact rupture between liquid and post is significantly affected by dynamic effects [21]. In particular, the dynamics

controls the transition between pure dewetting and liquid bridge rupture. Indeed in all the numerical cases studied here, contact line depinning actually proceeds by dewetting from the post surface. This process is characterized by a complex dynamics, involving confinement both in the elongated meniscus and at the contact line. This dissipation is bound to effectively increase the work of adhesion.

To date, receding contact angles have been modeled through the depinning of straight line segments only [12,13,22]. However, our results demonstrate that it is the depinning of the kinks in the line which controls the dynamics. It is well known that suitable defects may lower deformation thresholds: in the Peierls-Nabarro mechanism [23,24], for instance, dislocations set the threshold for plastic yielding in crystalline materials.

Similarly a wide variety of systems ranging from magnetic domain walls to DNA chains can be viewed as elastic chains coupled to a periodic lattice. The dynamics of the chains is controlled by the kinks which emerge from the competition between periodic lattice interaction and elastic coupling between segments: this is the Frenkel-Kontorova model [25]. A contact line moving on a periodic array is simply another type of elastic chain coupled to a lattice. The interaction with the lattice is mediated by the liquid meniscus adherent to the post (Fig. 4). It is affected by the shape of the post and also, if the post is not circular, by its orientation relative to the contact line. In the kink, the conformation of the line itself is directed by the underlying lattice so that altogether, the local geometry of the post array is expected to affect the coupling of the chain to the lattice. Historically the plastic deformation of crystalline materials has thoroughly been understood once the preferential slip planes and directions for dislocations have been rationalized in terms of lattice symmetries [26]. Likewise we can expect that with the kink concept, receding contact angles can be rationalized in terms of symmetry of the post arrays.

In conclusion, we have evidenced that kinks in receding contact lines are the relevant elementary mechanism of motion on periodic superhydrophobic surfaces. Simulations fully vindicate the role of the kinks in the quasistatic motion of the contact line: they account for both wetting isotropy and reduction of the depinning threshold. Contact lines are yet another example of Frenkel-Kontorova chains and based on the abundant literature [25] we expect that the kink concept can lead to a rationalization of the dependence of receding contact angles on underlying surface geometry. As a next step, the dissipative processes should also be taken into account including fluid viscosity both at the meniscus scale and at smaller length scales near the contact line.

We thank M. Gorynsztejn-Leben for suggesting the post loop experiment. We acknowledge support from the National Research Agency (ANR, DYNALO Project No. NT09 499845).

- [1] D. Öner and T. J. McCarthy, Langmuir 16, 7777 (2000).
- [2] D. Quéré, Physica (Amsterdam) 313A, 32 (2002).
- [3] A. Marmur, Langmuir 20, 3517 (2004).
- [4] A. Tuteja, W. Choi, J. Mabry, G. McKinley, and R. Cohen, Proc. Natl. Acad. Sci. U.S.A. 105, 18 200 (2008).
- [5] Y. Y. Yan, N. Gao, and W. Barthlott, Adv. Colloid Interface Sci. 169, 80 (2011).
- [6] A. B. D. Cassie, Discuss. Faraday Soc. 3, 11 (1948).
- [7] P. de Gennes, Rev. Mod. Phys. 57, 827 (1985).
- [8] L. Gao and T. McCarthy, Langmuir 22, 6234 (2006).
- [9] S. Moulinet, C. Guthmann, and E. Rolley, Eur. Phys. J. E 8, 437 (2002).
- [10] J. Schmittbuhl and K. J. Måløy, Phys. Rev. Lett. 78, 3888 (1997).
- [11] E. Barthel, G. Kriza, G. Quirion, P. Wzietek, D. Jérome, J. B. Christensen, M. Jørgensen, and K. Bechgaard, Phys. Rev. Lett. 71, 2825 (1993).
- [12] C. Extrand, Langmuir 18, 7991 (2002).
- [13] W. Choi, A. Tuteja, J. Mabry, R. Cohen, and G. McKinley, J. Colloid Interface Sci. 339, 208 (2009).
- [14] N. Patankar, Langmuir **26**, 7498 (2010).
- [15] C. Dorrer and J. Rühe, Langmuir 22, 7652 (2006).

- [16] A. Dubov, J. Teisseire, and E. Barthel, Europhys. Lett. 97, 26003 (2012).
- [17] C. Priest, T. Albrecht, R. Sedev, and J. Ralston, Langmuir 25, 5655 (2009).
- [18] W. Xu and C.H. Choi, Phys. Rev. Lett. **109**, 024504 (2012).
- [19] See Supplemental Material at http://link.aps.org/supplemental/10.1103/PhysRevLett.110.046101 for a video of the contact line kinematics.
- [20] K. Brakke, Exp. Math. 1, 141 (1992).
- [21] R. Dufour, P. Brunet, M. Harnois, R. Boukherroub, V. Thomy, and V. Senez, Small 8, 1229 (2012).
- [22] B. M. Mognetti and J. M. Yeomans, Langmuir 26, 18162 (2010).
- [23] R. Peierls, Proc. Phys. Soc. London **52**, 34 (1940).
- [24] F.R.N. Nabarro, Proc. Phys. Soc. London 59, 256 (1947).
- [25] O. Braun and Y. Kivshar, *The Frenkel-Kontorova Model: Concepts, Methods, and Applications* (Springer, New York, 2004).
- [26] D. Hull and D.J. Bacon, *Introduction to Dislocations* (Butterworth-Heinemann, Oxford, UK, 1965).